SAE International Journal of Commercial Vehicles

Comparative Analysis of Emergency Evasive Steering for Long Combination Vehicles

--Manuscript Draft--

Manuscript Number:	02-13-03-0018
Full Title:	Comparative Analysis of Emergency Evasive Steering for Long Combination Vehicles
Short Title:	Comparative Analysis of Emergency Evasive Steering for Long Combination Vehicles
Article Type:	Original Article
Corresponding Author:	Yang Chen, Ph.D Center for Vehicle Systems and Safety Blacksburg, VA UNITED STATES
Corresponding Author Secondary Information:	
Corresponding Author's Institution:	Center for Vehicle Systems and Safety
Corresponding Author's Secondary Institution:	
First Author:	Yang Chen, Ph.D
First Author Secondary Information:	
Order of Authors:	Yang Chen, Ph.D
	Zichen Zhang, Bachelor degree
	Mehdi Ahmadian, PhD

02-13-03-0018

Comparative Analysis of Emergency Evasive Steering for Long Combination Vehicles

Abstract

This study provides a simulation-based comparative analysis of the distance and time needed for long combination vehicles (LCVs)—namely, A-doubles with 28-, 33-, and 48-ft trailers—to safely exercise an emergency, evasive steering maneuver such as required for obstacle avoidance. The results are also compared with conventional tractor-semitrailers with a single 53-ft trailer. A multi-body dynamic model for each vehicle combination is developed in TruckSim® with an attempt to assess the last point to steer (LPTS) and evasive time (ET) at various highway speeds under both dry and wet road conditions. The results indicate that the minimum avoidance distance and time required for the 28-ft doubles vary from 206 ft (60 mph) to 312 ft (80 mph) and 2.3s to 2.6s, respectively. The required LPTS represents a 6 to 31% increase when compared with 53-ft semitrucks. When driving below 76 mph on a dry road and below 75 mph on a wet road, the 28-ft doubles exhibit LPTS and ET that are larger than 33-ft doubles. In addition, the 33-ft doubles exhibit larger LPTS and ET than 48-ft doubles for the highway speeds considered. This is mainly attributed to the longer trailer wheelbase that causes smaller rear trailer amplifications. At speeds higher than 76 mph on dry roads and 75 mph on wet roads, however, an opposite trend is observed. As the trailer length increases, the distance and time needed to safely avoid an obstacle also increase. A comparison between dry and wet road conditions is also conducted, with the results indicating that more time and distance would be needed for obstacle avoidance on wet roads.

Keywords: Long Combination Vehicles, LCVs, obstacle avoidance, highway speed, A-double, multi-trailer truck, TruckSim, the last point to steer, emergency maneuvering

1. Introduction

An area of concern for commercial vehicles in general, long combination vehicles (LCVs) in particular is the ability to safely maneuver the vehicle to avoid obstacles at highway speeds. The U.S. Department of Transportation (DOT) reports that in 2017, there were 4,237 fatal and 102,000 highway injuries and crashes, respectively, involving large trucks. The DOT data indicates that 94.6% of injuries and 95.3% of crashes occurred as a result of colliding with a fixed object, slowing or stopped vehicles, pedestrians, animals, and other objects [1]. In the same year, 4,102 persons were killed in commercial truck-related crashes, 64% of which were associated with LCVs [1, 2].

To reduce vehicle collisions, some passenger vehicles and commercial trucks are equipped with collision warning and emergency steer assist (ESA) systems. The implementation of ESA commercial vehicles is often more complex because of the added challenges associated with larger gross vehicle weights of the vehicle, length, and more complex roll and yaw dynamics. Better understanding the requirements for safely maneuvering commercial vehicles in emergency conditions would be helpful with developing of such safety systems, in addition to providing a better appreciation of the complexities of obstacle avoidance maneuvers in LCVs.

This paper aims to provide a simulation analysis of the last-point-to-steer (LPTS) and evasive-time (ET) that are often adopted as the critical factors in triggering a collision-avoidance system or steering maneuver by the driver. The study will include various types of LCVs that are commonly operated in North America, such as 28-, 33-, and 48-ft A-doubles. The results are compared with the conventional 53-ft semitrucks for both dry and wet road conditions.

2. Background and Technical Reviews

2.1 Last Point to Steer (LPTS)

The last point to steer (LPTS) refers to the last possible position to avoid the obstacle through steering or taking evasive action [3]. Before attaining the LPTS, the warning and ESA systems are supposed to kick in, enabling the driver to safely steer past the obstacle [4]. A study conducted by Eckert et al. [5] indicates that for a passenger car, the minimum distance to steer increases linearly to the speed, while the minimum distance to brake increases proportionally to the square of the speed, as shown in Figure 1. This implies that evading by steering is more efficient than braking when driving on highways (i.e. at high speeds). By contrast, braking is more desirable in urban situations (i.e. at low speeds).

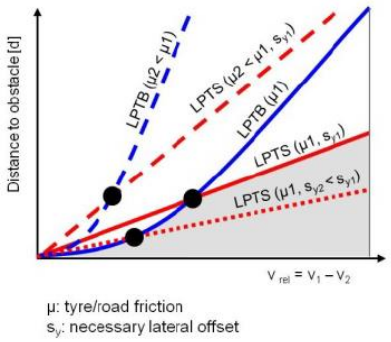

Last point to brake (LPTB):

$$d_b = -\frac{1}{2\,a_x} * v^2{}_{rel}$$

Last point to steer (LPTS):

$$d_e = \sqrt{\frac{2\,s_y}{a_y}} * v_{rel}$$

Figure 1. Minimum distance to avoid a collision by braking or steering [5]

Figure 2 outlines the last point to steer (LPTS) and the last point to brake (LPTB) in high-speed driving conditions, in which the LPTS is located closer to the obstacle than the LPTB. The driver can avoid the crash by evading maneuvers in spite of missing the LPTB. However, if the vehicle goes beyond the LPTS, a collision will be inevitable. Therefore, the LPTS is the critical threshold of provoking the warning or ESA systems in high-speed driving conditions. Shiller et al. [3] point out that the LPTS is correlated with the minimum longitudinal displacement in emergency lane-change maneuvers subject to vehicle dynamics, steering rate, and tire forces. In addition, the study conducted by Eckert et al. indicates that the LPTS increases due to lower road friction or more necessary lateral offset, shown in Figure 1.

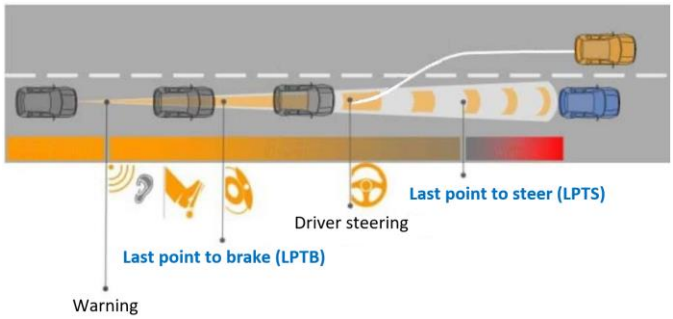

Figure 2. The last point to steer/brake at high-speed driving conditions [5]

2.2 Evasive Time (ET)

The other method widely adopted by collision avoidance systems to make a decision is to employ the time interval, mainly including the time to steer (TTS), the time to collision (TTC), and the evasive time (ET) [6]. The TTS is the time after which an evasive maneuver must be executed to dodge the obstacle. When the TTS reaches zero, the collision cannot be avoided by steering. A study from Ackermann et al. indicates that the TTS is a function of the TTC and the ET for a passenger car [7]:

$$TTS = TTC - ET - t_l = \frac{d_d}{V_{x1}} - \frac{LPTS}{V_{x1}} - t_l = \frac{d_d}{V_{x1}} - \sqrt{\frac{2s_y}{a_y}} - t_l \qquad (1)$$

where the time-to-collision (TTC) is the time needed to collide with the obstacle, which can be calculated by dividing the distance to the obstacle (d_d) over the present driving speed (V_{x1}) [8-10], the evasive time (ET) is the time-to-collision from the last point to steer, and t_l is the steering loss time. Typically, the evasive time (ET) in eq. (1) is the theoretical and absolute minimum time needed for activating a collision-avoidance system. In practice, as much as twice this time is needed for safely avoiding an obstacle, in order to account for the system and vehicle delays that inevitably exists.

It is important to notice that entire previous studies pertaining to the last point to steer (LPTS) and the evasive time (ET) are associated with the single-unit vehicle, which may make their results inapplicable for multi-trailer trucks. Thus, this paper proposes modeling and simulation to investigate the last point to steer (LPTS) and the evasive time (ET) in high-speed driving conditions for multi-trailer trucks.

2.3 Multi-trailer Trucks

In the past decades, various combinations of multiple trailers have been used with increasing frequency on U.S. highways due to the rapid increase of E-commerce cargo transport demands. This study focuses on the combination of A-double trailers on the tractor (also referred to as "A-train" or "A-double"), which is the most prevalent combination and has been widely adopted by many U.S. fleets in their operations. The double-trailer trucks provide operational advantages in terms of loading and uploading, ease of distribution, and other key logistics that are superior to the conventional 53-ft trailers that are commonly used for bulk cargo over long hauls [11]. As shown in Figure 3, the two trailers are linked together by a converter A-dolly. The dolly is hooked up to a pintle hitch on the rear of the front trailer while connecting to the rear trailer by a fifth-wheel coupling. The pintle hitch can be approximated to be a spherical joint providing three rotational degrees of freedom in the normal operating range [12]. The fifth wheel coupling allows for free yaw rotational motion, but limited roll and pitch rotational motions. Both pintle hitch and fifth-wheel couplings are under translation constraints in all three directions. Those articulation points enhance the flexibility of vehicle motion, but diminish the vehicle dynamic stability, posing additional safety risks, especially in emergency evasive maneuvers.

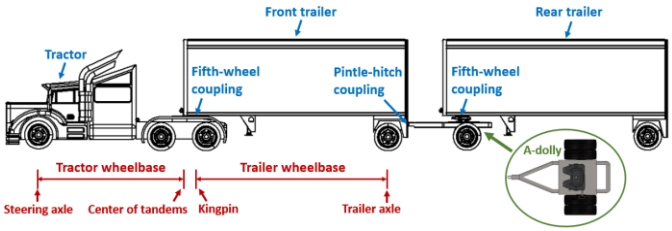

Figure 3. Double-trailer truck with the use of A-dolly

A dynamic that occurs in LCVs is the rearward amplification of the rear trailer, commonly referred to as the "crack-the-whip" response [13]. This phenomenon is the tendency of the trailing unit to laterally over-respond during a rapid high-speed evasive maneuver. The rearward amplification is believed to be the primary cause of excessive sway and rollover in the rearmost trailer of a long combination vehicle [14]. Winkler [15] reported that the rearward amplification of the A-double is a strong function of maneuver frequency and tends to peak during quick and evasive maneuvers, such that the truck is quite susceptible to rollover of the last trailer. MacAdam [16] found that in many large combination vehicles, the rearward amplification problem is more likely to occur when traveling at highway speeds above 50 mph.

Another issue that such long vehicles ordinarily encounter is a phenomenon named off-tracking. Off-tracking is when the rear trailer axle travels in a different path from the path of the tractor steering axle [17]. In the context of a high-speed lane change, the last trailer that experiences transient off-tracking travels inward, subsequently outward of the tractor path [14]. This transient off-tracking is undesired during evasive maneuvers, since it may cause the last trailer to hit the obstacle or run off the road. Hence, the rearward amplification and off-tracking effects must be considered in the study of emergency evasive maneuvers for long combination vehicles.

3. Double-trailer Dynamic Models

For this study, vehicle dynamic models for 28-ft double, 33-ft double, 48-ft double, and 53-ft single trailer trucks are developed using TruckSim to represent those commonly operated on U.S. highways. The TruckSim model is then validated by comparing the simulation results of the TruckSim model with those obtained from a lateral and yaw dynamic model (mathematical model) developed in Simulink as well as the data collected during physical tests on test-tracks.

3.1 Lateral and Yaw Dynamic Model

The lateral and yaw dynamic behavior of articulated heavy vehicles can be described by a yaw-plane single-track dynamic model, which has been widely used in numerous literatures such as [18-21]. A schematic diagram of the yaw-plane single-track dynamic model for a six-axle A-double is shown in Figure 4, which consists of four vehicle units (tractor, front trailer, dolly, and rear trailer). Each vehicle unit is considered as a sub-model. The mathematical equations that govern the lateral and yaw dynamic behavior of each sub-model are derived based on Newton's Second Law.

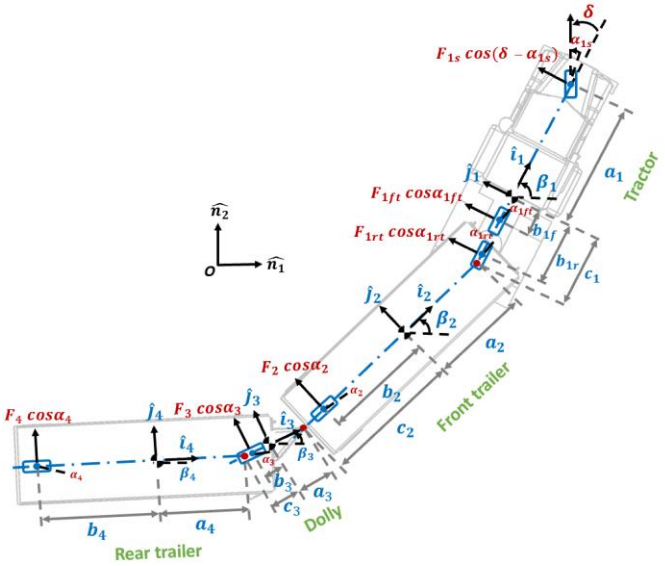

Figure 4. Schematic diagram of the A-double combination vehicle

3.1.1 Tractor Dynamic Sub-model

The lateral and yaw equations of motion for the tractor, as shown in Figure 5, are derived by force balance in the lateral direction and moment balance at the center of gravity (CG) of the vehicle, as:

$$m_1\left(\dot{V}_{y1} + \dot{\beta}_1 V_{x1}\right) = F_{1s}\cos(\delta - \alpha_{1s}) + F_{1ft}\cos\alpha_{1ft} + F_{1rt}\cos\alpha_{1rt} - F_{y1}\cos(\beta_1 - \beta_2) \quad (2)$$

$$I_1\ddot{\beta}_1 = a_1 F_{1s}\cos(\delta - \alpha_{1s}) - b_{1f}F_{1ft}\cos\alpha_{1ft} - b_{1r}F_{1rt}\cos\alpha_{1rt} + c_1 F_{y1}\cos(\beta_1 - \beta_2) \quad (3)$$

where V_{x1} and V_{y1} are the longitudinal and lateral velocities, β_1 and β_2 are the yaw angles of the tractor and the front trailer, F_{1s}, F_{1ft}, and F_{1rt} are the tire cornering force (perpendicular to the tire traveling direction), a_1, b_{1f}, b_{1r}, and c_1 are the distance from CG to the steering axle, the front drive axle, the rear drive axle and the fifth wheel coupling, respectively, m_1 and I_1 denote the tractor's mass and yaw moment of inertial, F_{y1} is the lateral force at the articulation point, which needs to be provided by the front trailer sub-model, δ is the steering angle at the wheels, α_{1s} represents the tire slip angle at the steering axle, which can be calculated by:

$$\alpha_{1s} = \delta - tan^{-1}\left(\frac{V_{y1}+\dot{\beta}_1 a_1}{V_{x1}}\right) \quad (4)$$

For the slip angle at the front and rear drive axles:

$$\alpha_{1ft} = -tan^{-1}\left(\frac{V_{y1}-\dot{\beta}_1 b_{1f}}{V_{x1}}\right) \quad (5)$$

$$\alpha_{1rt} = -tan^{-1}\left(\frac{V_{y1}-\dot{\beta}_1 b_{1r}}{V_{x1}}\right) \quad (6)$$

The slip angle is used to calculate the cornering force by a lookup table, which will be discussed later in Section 3.2.2. It should be noted that the forward velocity V_{x1} is considered at a constant value in the present study. Therefore, the longitudinal dynamic equation of motion is ignored for simplification.

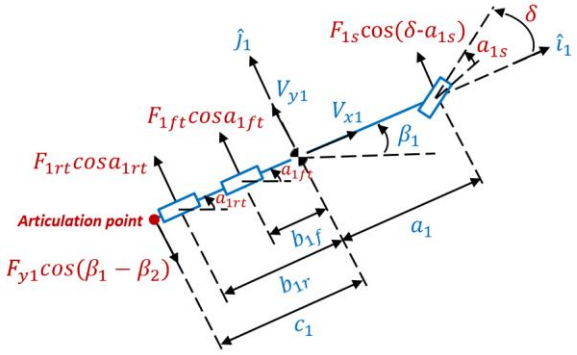

Figure 5. Schematic diagram of the tractor

3.1.2 Trailer and Dolly Dynamic Sub-models

Similarly, the lateral and yaw equations of motion for the trailer and the dolly, as shown in Figure 6, can be written as:

$$m_i\left(\dot{V}_{yi} + \dot{\beta}_i V_{xi}\right) = F_{y(i-1)} + F_i\cos\alpha_i - F_{yi}cos(\beta_i - \beta_{i+1}) \quad (7)$$

$$I_i\ddot{\beta}_i = a_i F_{y(i-1)} - b_i F_i\cos\alpha_i + c_i F_{yi}\cos(\beta_i - \beta_{i+1}) \quad (8)$$

where the subscript letter *i=2,3,4* denotes the front trailer, the dolly, and the rear trailer, respectively. For the rear trailer that does not tow any additional vehicle, the term associated with $F_{yi}cos(\beta_i - \beta_{i+1})$ should be removed in both eq. (7) and (8). The slip angle, α_i (*i=2,3,4*) for the front trailer, the dolly, and the rear trailer can be obtained by:

$$\alpha_i = -tan^{-1}\left(\frac{V_{yi}-\dot{\beta}_i b_i}{V_{xi}}\right) \quad (9)$$

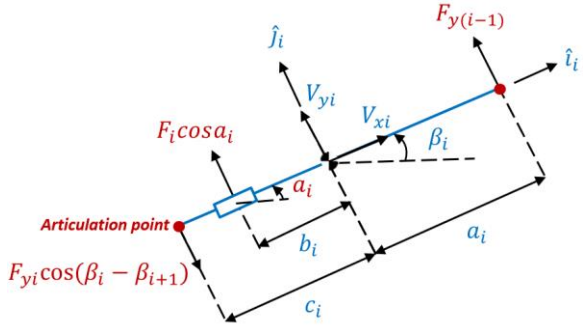

Figure 6. Schematic diagram of the front trailer, the dolly, and the rear trailer

3.1.3 Combined Model in Simulink

Kinematic constraints at articulation points are applied to combine the towing and towed vehicle sub-models. The translational velocities of the towed vehicle can be derived from the velocities and yaw rate of the towing vehicle. Translational velocities at the articulation point can be written in the towing vehicle coordinate as:

$$V_{art(i-1)} = V_{x(i-1)}\hat{\imath}_{i-1} + (V_{y(i-1)} - c_{i-1}\dot{\beta}_{i-1})\hat{\jmath}_{i-1} \quad (10)$$

where $V_{art(i-1)}$ $(i=2,3,4)$ represents the translational velocities at the first, second, and third articulation point in the combination vehicle. By multiplying the vector rotation matrix:

$$\begin{bmatrix}\hat{\imath}_i \\ \hat{\jmath}_i\end{bmatrix} = \begin{bmatrix}\cos(\beta_{i-1}-\beta_i) & -sin(\beta_{i-1}-\beta_i) \\ \sin(\beta_{i-1}-\beta_i) & \cos(\beta_{i-1}-\beta_i)\end{bmatrix}\begin{bmatrix}\hat{\imath}_{i-1} \\ \hat{\jmath}_{i-1}\end{bmatrix} \quad (11)$$

The translational velocities of the vehicle CG are obtained in the towed vehicle coordinate, which is a function of the velocities of the towing vehicle as:

$$V_{xi} = V_{x(i-1)}\cos(\beta_{i-1}-\beta_i) - (V_{y(i-1)} - c_{i-1}\dot{\beta}_{i-1})\sin(\beta_{i-1}-\beta_i) \quad (12)$$

$$V_{yi} = V_{x(i-1)}\sin(\beta_{i-1}-\beta_i) + (V_{y(i-1)} - c_{i-1}\dot{\beta}_{i-1})\cos(\beta_{i-1}-\beta_i) - \dot{\beta}_i a_i \quad (13)$$

According to eq. (2)-(13), a double-trailer dynamic model is developed in Simulink, as shown in Figure 7. The Simulink model includes four sub-models in representative of tractor, front trailer, dolly, and rear trailer. The towed vehicle sub-model receives the longitudinal and lateral velocities and the yaw angle from the towing vehicle sub-model, while feeding the articulation force back to the towing vehicle unit. Steering angle and driving speed are the input of the model. The Simulink dynamic model will be used to validate the model developed in TruckSim, as discussed in the following section.

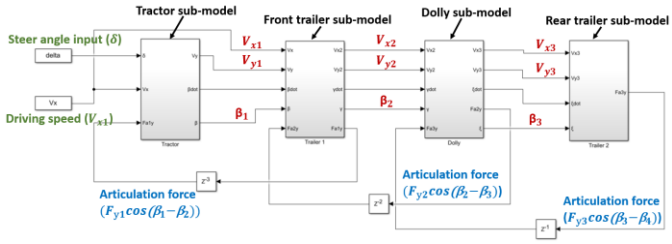

Figure 7. Double-trailer lateral and yaw dynamic model in Simulink

3.2 TruckSim Model Development

TruckSim is a commercially available software well recognized for providing accurate and realistic motion predictions for dynamic models of various commercial truck combinations. Those models include the compliant effects of tire and suspension systems, and three-dimensional (3-D) multi-body dynamics of articulated vehicles. For this study, vehicle dynamic models of 28-ft double, 33-ft double, 48-ft double, and 53-ft single trailer combinations are established using TruckSim, as shown in Figure 8. Basic dimensional parameters for the TruckSim simulation, such as wheelbase, axle track, suspension lateral spacing, etc., are identified by direct measurements on real trucks. For some parameters related to braking, power transmission, etc. are difficult to determine, TruckSim default values are applied. To ensure the accuracy and effectiveness of the model in the scope of this study, the model inputs associated with vehicle dimensional inertial (CG) properties and tire cornering force characteristics are calibrated through other simulation tools and test data.

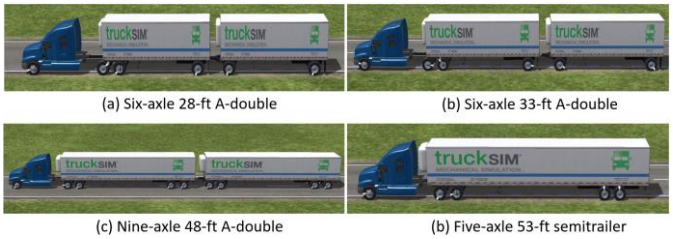

Figure 8. Tractor-trailer combination vehicle models in TruckSim

3.2.1 Vehicle Dimensional Inertial (CG) Properties Setup

The specific CG and inertial properties for the tractor and A-dolly can be found in references [22, 23]. The weight and inertial properties of the 28-ft and 33-ft trailers are identified through CAD models created in SolidWorks, as shown in Figure 9. the CAD model captures all structural features and includes material property (density) for each component. A blue cuboid is placed inside the trailer to represent the normal highway loading condition. The load is assumed to be fixed to the trailer, having a uniform density and occupying 80% inner volume of the trailer. In addition, the parameters necessary for the 53-ft and 48-ft trailer simulations are referred from literatures [24-26].

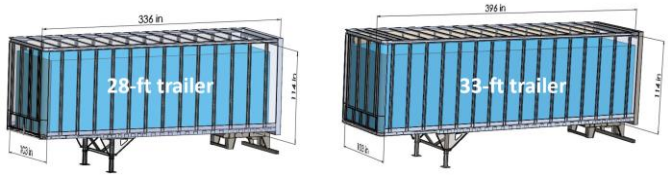

Figure 9. CAD models of 28-ft and 33-ft trailers in SolidWorks

3.2.2 Tire Cornering Force Characteristics Determination

To Simulate the lateral and yaw dynamics of the vehicle requires knowledge of tire cornering force characteristics. The cornering force, known as the tire-road lateral force, is greatly affected by slip angle (α_k) and tire vertical load (F_{zk}) [27], which can be expressed as:

$$F_k = f(F_{zk}, \alpha_k) \quad (14)$$

where F_{zk} is the tire vertical load and α_k is the tire slip angle, the subscript letter $k=1s,1ft,1rt,2,3,4$ for the axles from the tractor to the rear trailer. To reasonably represent the cornering force characteristics, the test data of the truck tire (Michelin 11R22.5) obtained from the University of Michigan Transportation Research Institute (UMTRI) [28] is applied in the current work, as shown in Figure 10. Based on the test data, a lookup table is established to calculate the cornering force with the inputs of slip angle and tire vertical load, which is then integrated into the tire models of TruckSim model and the dynamic model previously developed in Section 3.1.

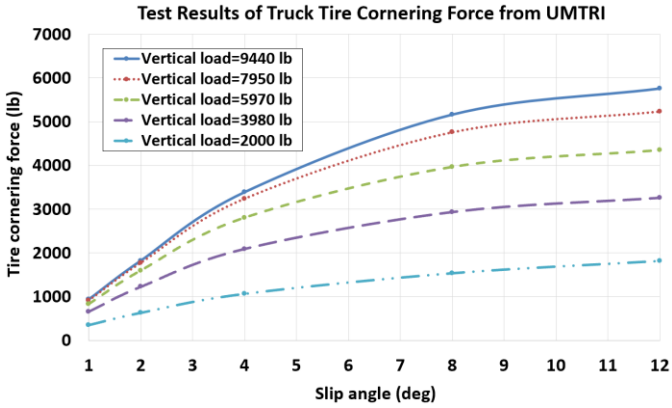

Figure 10. Test results of truck tire cornering force from University of Michigan Transportation Research Institute (UMTRI) [28]

With the given tire cornering force characteristics (in Figure 10), a similarity method that was proposed by Pacejka [29] is used to calculate the cornering force for different road friction coefficients:

$$F_k = \frac{\mu}{\mu_0} f(F_{zk}, \frac{\mu_0}{\mu}\alpha_k) \quad (15)$$

where μ is the road friction coefficient, μ_0 is the tire measurement friction coefficient that is given in [28]. Figure 11 shows the tire cornering force curves for various road friction coefficients under a constant tire vertical load of 5970 lb. As noted there, a higher road friction coefficient results in an increase in the tire cornering stiffness,

i.e. for the case of a lower road friction coefficient, there is necessity to develop more tire slip angles to generate the cornering force, which would result in a larger sway in the last trailer during the lane change.

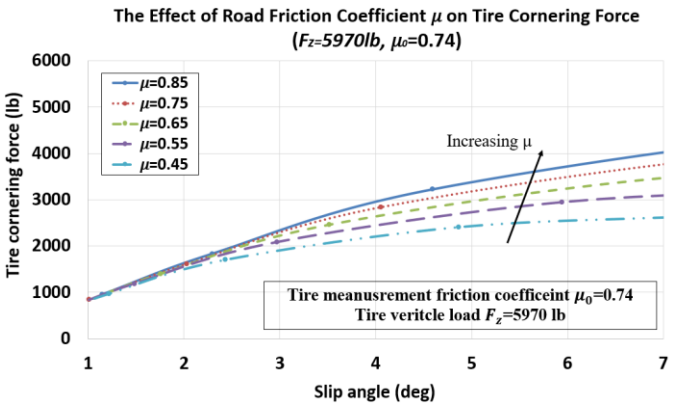

Figure 11. The effect of road friction coefficient on the tire cornering force characteristic (tire vertical load=5970 lb)

3.3 Validation of the TruckSim Model of 28-ft Doubles

The TruckSim model yields simulation results, which are validated by comparing with those obtained from the corresponding dynamic model developed in Section 3.1 as well as the measured data from physical tests on test-tracks. The validation mainly focuses on the 28-ft A-double truck model, since the tractor, dolly, suspension, tires, etc. in the other vehicle models are the same as those used in the 28-ft doubles model. For comparison purpose, the truck loading condition (load=6000 lb) considered in the field test is applied in the simulation of this section. Table A1 in Appendix A lists the parameters used for the model validation in this section. It needs to be clarified that this load condition is different from the one used in the simulation study of Section 4, in which all combination vehicles are loaded to their federal maximum gross weight limit.

3.3.1 Comparison with the Lateral and Yaw Dynamic Model in Simulink

To compare the dynamic responses of the TruckSim model and the Simulink dynamic model of the 28-doubles, a single lane change at a constant speed of 45 mph is simulated. For comparison purpose, the average left and right wheel steering angles from the TruckSim model is applied as the input to the Simulink model, as shown in Figure 12.

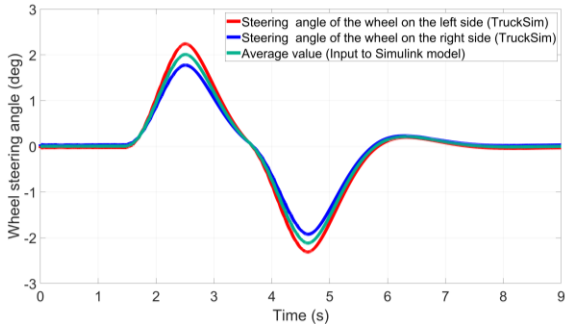

Figure 12. The average of left and right wheel steering angles from the TruckSim model is applied to the dynamic model in Simulink for a single lane change at 45 mph

Figure 13 shows the comparison results between the two models in terms of yaw rates, lateral accelerations and articulation angles of tractor and trailers. As indicated, the dynamic responses of the two models are very close for the single lane change maneuver and speed considered. This agreement verifies the capacity of the TruckSim model in capturing the lateral and yaw dynamic behavior of the double-trailer truck.

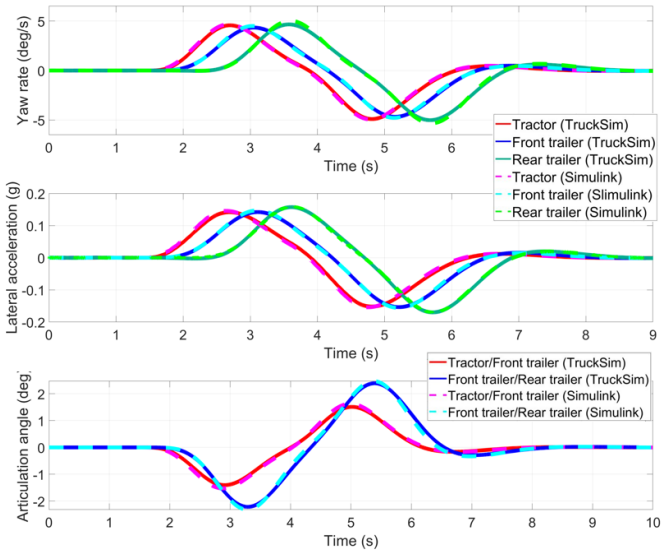

Figure 13. Comparison of yaw rates, lateral accelerations, and articulation angles between the TruckSim model and Simulink developed dynamic model for a single lane change at 45 mph

3.3.2 Comparison with Field Test Results

Data collected in the truck field tests, which were conducted by the Center for Vehicle Systems and Safety (Virginia Tech) at Michelin Laurens Proving Grounds (MLPG), are also applied to validate the dynamic model in TruckSim. The testing vehicle is an A-double that consists of a 2004 Volvo VNL tractor and two van trailers with the length of 28-ft. Safety equipment such as outriggers was equipped to keep the test driver safe while preserving the testing vehicle during roll stability test maneuvers, as shown in Figure 14. In particular, a load frame was designed and installed in the trailer to achieve the CG inertial requirement for the normal highway loading condition, which has been discussed in a previously published paper [14].

Figure 14. Outrigger-integrated 28-ft A-double in test field

LiDAR sensors (LeddarTech M16) were mounted on the back of the tractor as well as on the front of the rear trailer to measure the articulation angles between the tractor and the front trailer, and between the front and rear trailers. In addition, accelerometers (PCB 3713D1FD3G) were installed nearby the position of the vehicle CG to sense the accelerations in three directions for the tractor, the front trailer, and the rear trailer. A second order lowpass Butterworth filter with a cutoff frequency of 2 Hz was used to clean up the test raw data (sampling rate = 125 Hz). For the comparison between the simulation and the cleaned test data, the test results of steering wheel angel and driving speed for a double-lane-change maneuver (operated by a skilled driver) are applied to the TruckSim model as the input. The comparison results are shown in Figure 15, which indicates a good

agreement between the simulation and test data in lateral accelerations and articulation angles of tractor and trailers. This consistency verifies the ability of the developed TruckSim model in accurately predicting lateral and yaw dynamic responses of tractor and trailers during lane-change maneuvers.

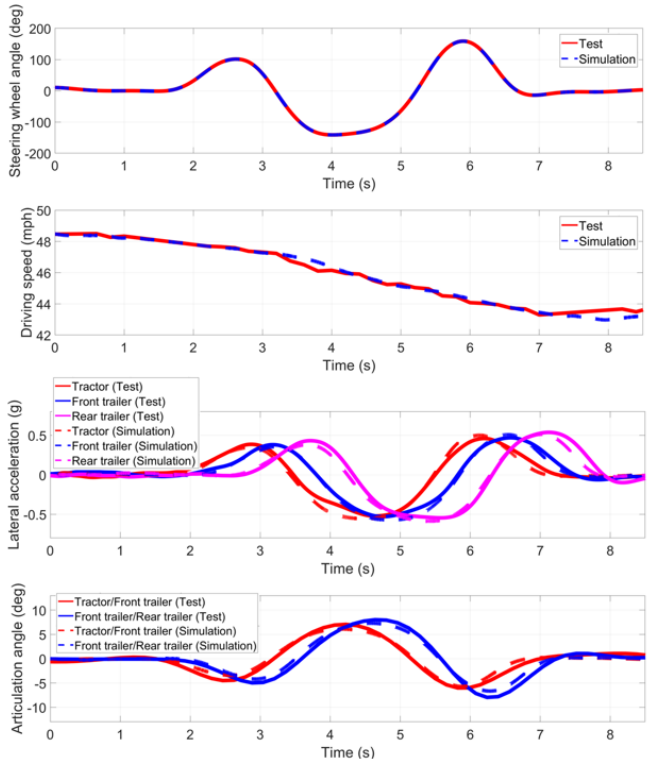

Figure 15. Comparison of steering wheel angle, driving speed, lateral acceleration, and articulation angle between TruckSim simulation and test results for a double lane-change maneuver

3.4. Trajectory Calculation of Trailer Rear Corner

It is important to note that during the emergency lane change maneuver, the last trailer must pass around the obstacle, while not swaying outward excessively and hitting obstacle roadside such as traffic barrier. Therefore, the yaw-plane trajectories of the last trailer's rear corners on both left and right sides need to be evaluated in the simulation. TruckSim is, however, not capable of providing the output of the trajectory of the trailer's body corner. Therefore, a model is developed in Simulink, which is coupled with TruckSim, to calculate the required trajectory. The calculation starts with locating the position of the point (point G in Figure 16) from the trailer's center of gravity (CG) by the position vector:

$$\vec{r} = -c_4\hat{\imath}_4 - s_4\hat{\jmath}_4 \tag{16}$$

where $\hat{\imath}_4$ and $\hat{\jmath}_4$ represent the Cartesian coordinate fixed to the vehicle body, c_4 is the distance from the CG to the rear of the last trailer, and s_4 is the half-width of the last trailer. The velocity of the point G in terms of the trailer's velocities and yaw rate can be written as:

$$\overrightarrow{v_G} = \left(V_{x4} + \dot{\beta}_4 s_4\right)\hat{\imath}_4 + \left(V_{y4} - \dot{\beta}_4 c_4\right)\hat{\jmath}_4 \tag{17}$$

where V_{x4} and V_{y4} are the last trailer's velocities in lateral and longitudinal directions, and $\dot{\beta}_4$ is the trailer yaw rate. By multiplying the vector transfer matrix:

$$\begin{bmatrix}\widehat{n_1}\\ \widehat{n_2}\end{bmatrix} = \begin{bmatrix}\cos\beta_4 & -sin\beta_4\\ \sin\beta_4 & \cos\beta_4\end{bmatrix}\begin{bmatrix}\hat{\imath}_4\\ \hat{\jmath}_4\end{bmatrix} \tag{18}$$

The velocity at point G in the global coordinate is obtained as:

$$\overrightarrow{v_G} = [\left(V_{x4} + \dot{\beta}_4 s_4\right)\cos\beta_4 - \left(V_{y4} - \dot{\beta}_4 c_4\right)\sin\beta_4]\widehat{n_1} + [\left(V_{x4} + \dot{\beta}_4 y\right)\sin\beta_4 + \left(V_{y4} - \dot{\beta}_4 c_4\right)\cos\beta_4]\widehat{n_2} \tag{19}$$

Integrating eq. (19) concerning the time produces the displacement of point G in the global coordinate. Although only trajectories of the rear corners on the left and right sides are needed for this study, eq. (16)-(19) are applicable for calculating the yaw-plane trajectory of any body-fixed point for each vehicle unit.

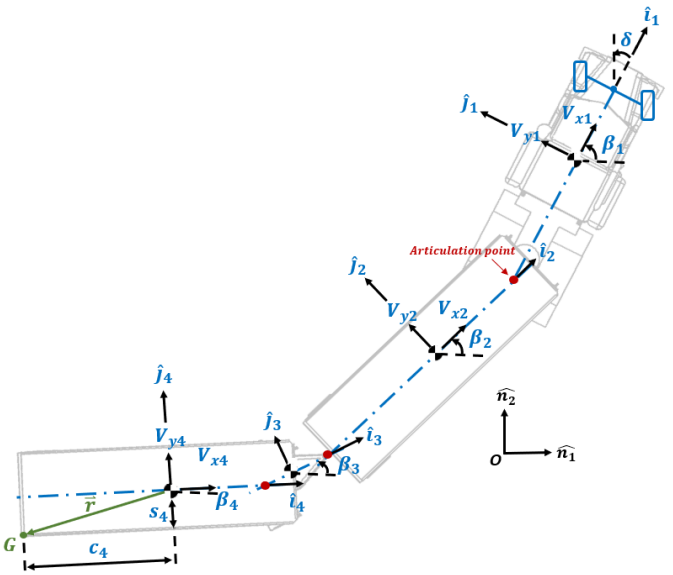

Figure 16. Yaw-plane model of an A-double combination

4. Simulation Study and Results Analysis

Based on the validated TruckSim model, extensive simulations are conducted to investigate the last point to steer (LPTS) and evasive time (ET) for the selected combination vehicles. In the simulation study, all combination vehicles are loaded to the federal maximum gross weight limit (80,000 lb.) enforced on interstate highways for comparison purpose [30]. The parameters used for the selected combination vehicle simulation are provided in Tables A2 and A3 of Appendix A. In addition, this study assumes the vehicle steering into the middle of the left-hand neighboring lane (road width=12ft) to avoid a fixed obstacle that fully blocks the forward path, as shown in Figure 17. The right lane change, if present, can be considered similarly. The forward speed is held at a constant value when driving and steering. The study considers the obstacle avoidance by steering solely, thereby excluding the brake contribution on evasive distance and time. The maximum achievable steering wheel rate of 250 deg/s is used based on a past study [31].

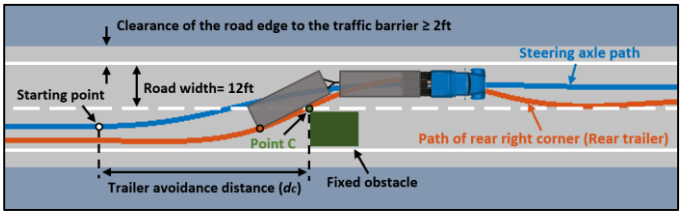

Figure 17. Illustration of an evasive maneuver for an A-double

As discussed earlier in Section 2.3, to identify the LPTS and the ET for long combination vehicles, it is necessary to consider the yaw and roll dynamic behavior of the last trailer. Thus, three requirements are introduced for the determination of emergency evasive maneuvers, which include:

1. The last trailer just happens to pass around the obstacle, i.e. the trailer's rear right corner passes through point C (in Figure 17), which is the point of intersection of the dashed white line (separating lanes of traffic) and the front line of the obstacle.
2. The rear left corner of the last trailer does not sway out of the road edge by 2 ft, which is the minimum clearance between the road edge and the highway traffic barrier [32].
3. Wheel lift-off does not occur in the last trailer axle(s).

4.1. Truck Dynamics Comparison and Simulation Analysis in Lane-change Maneuvers

To better understand the three requirements and to learn the trucks' dynamic responses in evasive maneuvers, a preliminary simulation is performed for the selected combination vehicles under a left-hand lane-change maneuver at the normal steering frequency of 0.25 Hz [33]. The speed is hold at a constant value of 65 mph. The specific path of the single lane change is shown in Figure 18.

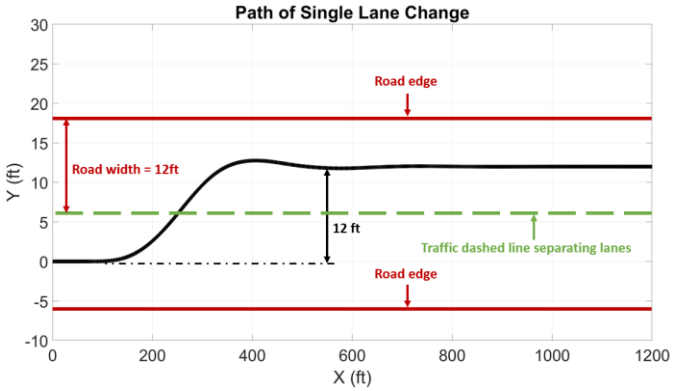

Figure 18. Path of single lane change

Figure 19 shows the simulation results of the lateral acceleration of tractor and rearmost trailer during the lane-change for the selected combination vehicles. The results indicate that the last trailer experiences a larger peak lateral acceleration than the tractor for each combination vehicle, which is the so-called rearward amplification phenomenon. The ratio of the peak lateral acceleration at the tractor and that on the trailing unit is generally utilized to gauge the rearward amplification [34]. As compared to the 53-ft single-trailer combination, a larger amount of rearward amplification is observed for the double trailer combinations, due to more yaw articulation points. More interestingly, the A-double combination with longer trailers has less rearward amplification due to their increased wheelbase providing extra stabilizing moments. The potential of the rearward amplification to cause an amplified path and a higher risk of rollover associated with the rearmost trailer is discussed in the following.

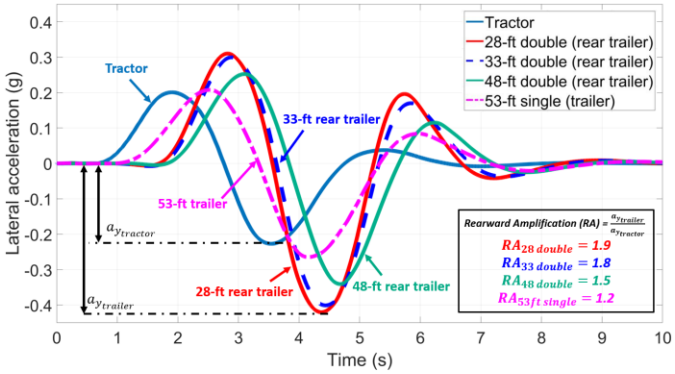

Figure 19. Time trace of the lateral acceleration of tractor and rearmost trailer for a lane change maneuver (speed=65 mph, friction coefficient=0.85)

Figure 20 shows the trajectories of the tractor steering axle center, the last trailer's axle center, and its rear corner on the left and right sides. By comparing the path between the steering axle center and the trailer's axle center, each combination vehicle exhibits an inboard off-tracking, followed by an outboard off-tracking during the lane change maneuver. The inboard off-tracking evaluation indicates that all points on the vehicle will clear the obstacle when the rear right corner of the rear trailer clears the obstacle. Therefore, the trajectory of the trailer's rear right corner is evaluated, and point C and distance d_c are defined as illustrated in Figure 17. It is assumed that the truck's lane of travel is fully blocked. Point C refers to the point of intersection of the dashed white line (separating lanes of traffic) and the front line of the obstacle. The d_c is associated with the trailer avoidance distance determined from the steering start point to point C. The shorter d_c (point C closer to the obstacle) the maneuver exhibits, the less ability the trailer possesses to avoid the obstacle. A magnifying lens is inserted in Figure 20 to better discriminate the point C location differences (resulting in different d_c) among the various truck combinations. As compared with A-doubles, the 53-ft single-trailer exhibits a shorter d_c, which implies that a higher steering rate is needed to avoid an obstacle. The 28-ft and 33-ft doubles have longer d_c than 48-ft doubles, indicating a better avoidance ability of the trailer. As compared with 33-ft doubles, 28-ft doubles have slightly shorter d_c.

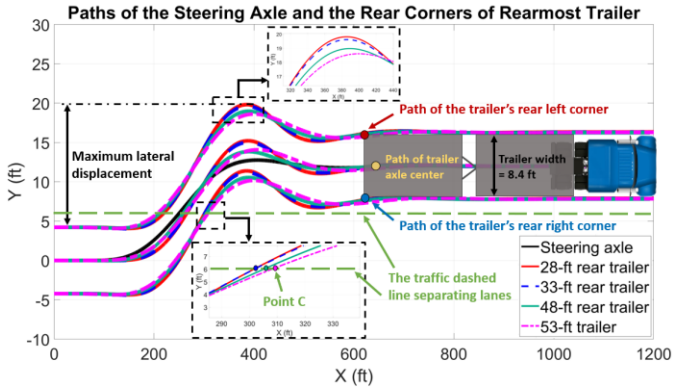

Figure 20. Paths of the steering axle and the last trailer's rear corners on both left and right sides for the lane change maneuver (speed=65 mph, friction coefficient=0.85)

Regarding the outboard off-tracking, the maximum lateral displacement of the trailer's rear left corner is used to evaluate the risk of collision with the traffic barrier. As indicated in the top zoomed-in inlay in Figure 20, the 28-ft trailer has the maximum lateral displacement of the last trailer's rear left corner slightly larger than the 33-ft trailer, followed by the 48-ft trailer. The 53-ft single trailer, with the smallest value of the maximum lateral displacement, is least likely to collide with the traffic barrier.

In the last, to assess the likelihood of rollover in the last trailer, a widely used metric, called the rollover index, is introduced. The rollover index is simply defined by the vertical load transfer on each tire divided by the total tire load on the driver and passenger sides [14, 35]:

$$\textit{Rollover Index (RI)} = \frac{F_{z_{right}} - F_{z_{left}}}{F_{z_{right}} + F_{z_{left}}} \qquad (20)$$

where $F_{z_{right}}$ and $F_{z_{left}}$ denote the total tire vertical loads on the driver and passenger sides, respectively. The absolute value of RI may vary from 0 at no load transfer to 1 at the event of wheel lift-off. Only simulation results on the rearmost trailer are presented here since in most cases the rear trailer is more prone to rollover than the front trailer during a quick and evasive maneuver. Figure 21 presents the time trace

of the rollover indices of the selected combination vehicles for the lane change maneuver. The results reveal that the rollover index peaks in the second turn during the lane change. The peak values of the rollover index of A-doubles are larger than 53-ft singles, due to the larger rearward amplification of the former. A-double trucks experience larger lateral accelerations, increasing the likelihood of a rollover. By comparing, longer trailers exhibit lower lateral acceleration peaks than shorter trailers due to their longer wheelbase [14, 26].

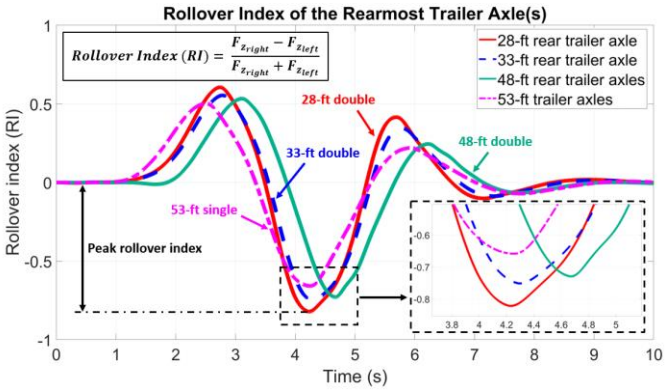

Figure 21. Time trace of rollover index for the lane change maneuver (speed=65 mph, friction coefficient=0.85)

The key findings of the preliminary simulation study are summarized as follows (> means larger than):

1. The chance of the last trailer collision with the obstacle that the driver attempts to avoid:
   53-ft single > 48-ft doubles > 33-ft doubles > 28-ft doubles
2. The last trailer's outward sway:
   28-ft doubles > 33-ft doubles > 48-ft doubles > 53-ft single
3. The likelihood of rollover in the last trailer:
   28-ft doubles > 33-ft doubles > 48-ft doubles > 53-ft single

4.2 LPTS and ET Determination at a Given Speed

Based on the preliminary simulation study, a strategy is proposed in this study to determine the last point to steer (LPTS) and the evasive time (ET) by TruckSim simulation and its specific steps are depicted in Figure 22. The last point to steer (LPTS) in the emergency maneuver can be found by minimizing d_c (i.e. increasing the lane-change intention) subject to yaw and roll motion limits in the last trailer (i.e. the second and third requirements). d_c is the distance from the maneuver starting point to point C, as previously discussed and illustrated in Figure 17. Figure 23 summarizes the maximum lateral displacement of the last trailer's rear left corner with respect to the distance (d_c) for the selected combination vehicles. As indicated, when the distance decreases (closer to the obstacle) to dodge the fixed obstacle in the forward path, a quicker movement with the steering wheel (a sharper maneuver) is performed, which in turn leads to a larger lateral movement in the last trailer. As compared to the 53-ft single-trailer truck, the maximum lateral displacement of A-double trucks is larger, and the difference tends to increase as the distance becomes shorter (quicker steering). This is mainly due to the greater amount of outboard off-tracking that the last trailer experiences, as previously discussed in Figures 20. In addition, less maximum lateral displacement is obtained for the A-double with longer trailers in the considered range of distance.

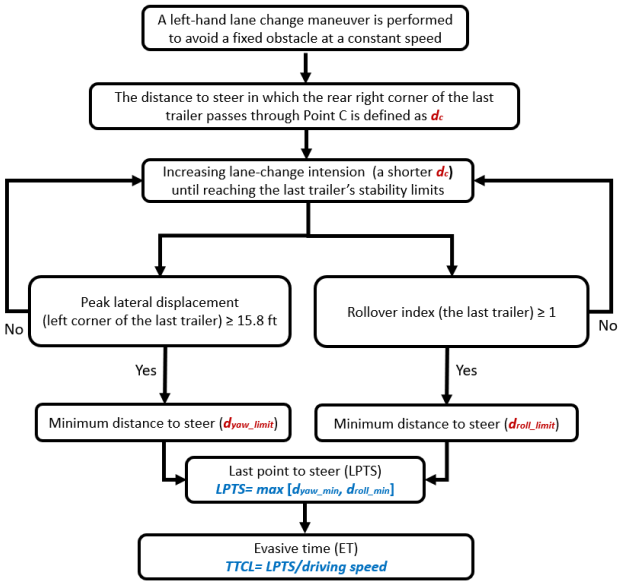

Figure 22. Flow chart for LPTS and TTCL determination

A minimum clearance of 2 ft between the road edge and the traffic barrier is considered in this study, resulting in an upper limit of 15.8 ft for the maximum lateral displacement shown in Figure 23. Corresponding to the upper limit, the minimum safe distance subject to the yaw motion limit of the last trailer (according to the second requirement) is determined, which is denoted by d_{yaw_limit}.

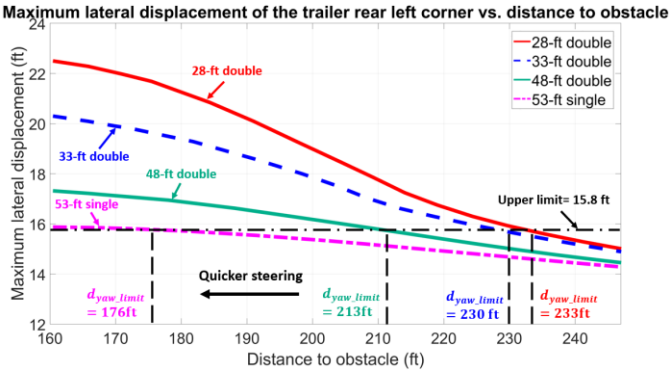

Figure 23. Maximum lateral displacement of the last trailer's rear left corner versus the distance to the obstacle (speed=65 mph, friction coefficient=0.85)

Figure 24 summarizes the peak values extracted from the rollover index (RI) for lane change maneuvers performed at various distances (d_c). The results in Figure 24 are quite consistent with those in Figure 23. The peak RI of 1 (wheel lift-off) is considered as the upper limit. Because over that value, the truck is involved in an unsafe situation with a strong tendency to roll over. When attaining the upper limit, the value in the X-axis is identified as the minimum safe distance to steer subject to the trailer roll dynamics limit (according to the third requirement), represented by d_{roll_limit}, as shown in Figure 24.

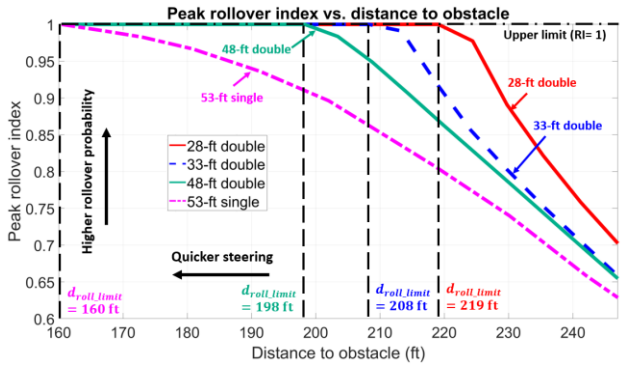

Figure 24. Peak rollover index of the last trailer versus the distance to the obstacle (speed=65 mph, friction coefficient=0.85)

Lastly, the last point to steer (LPTS) at the given speed (65 mph) is determined from the larger value between the d_{yaw_limit} and the d_{roll_limit} as:

$$LPTS = \max[d_{yaw\_limit}, d_{roll\_limit}] \quad (21)$$

By the driving velocity (V_{x1}), the evasive time (ET) can be obtained as:

$$ET = \frac{LPTS}{V_{x1}} \quad (22)$$

It is important to note that in this study all distances and times are without any steering or driver response delay. The driver response delay for the specific driving condition and any steering delay for the tractor must be added to the ET.

4.3 Summarized Results of LPTS and ET at Various Speeds

Based on the proposed approach, a batch of simulations are executed to evaluate the last point to steer (LPTS) and the evasive time (ET) for the single and double trailer combinations at various speeds. The friction coefficient is chosen as 0.85 and 0.50 for dry and wet asphalt roads, respectively [36]. Figures 25 and 26 compare the last point to steer (LPTS) among the selected combination vehicles for the dry and wet asphalt road conditions, respectively. The results indicate that as the speed increases, the value of LPTS increases for all combination vehicles for both road conditions. A larger rate of the LPTS to speed is observed for the A-double with longer trailers. Furthermore, as compared to the dry road condition, the wet road condition results in an increase of 5-31 ft in the LPTS. It is because the tire possesses a smaller cornering stiffness for the case of a lower road friction coefficient (as discussed in Figure 11). Consequently, during the lane change maneuver, the tires experience larger slip angles, resulting in an increase in the lateral sway of the rear trailer, which contributes to an increase in the LPTS. Overall, it can be concluded from the simulation results in Figures 25 and 26 that when the combination vehicles drive at a higher speed or on a lower-friction road due to rain or snow, a greater clearance distance is required for the obstacle avoidance maneuver in an emergency. In this regard, the warning and emergency steer assist (ESA) systems need to intervene earlier to guide the driver to swerve around the obstacle.

Additionally, in Figures 25 and 26, the A-doubles have the LPTS noticeably larger than that of the 53-ft single-trailer truck for entire considered speeds and both road conditions, due to the larger rearward amplification that the trailers experience. The LPTS for the 28-ft doubles is approximately from 206 ft to 307 ft on a dry road and from 215 ft to 312 ft on a wet road. At speeds below 76 mph for the dry road condition and below 75 mph for the wet road condition, the LPTS of the 28-ft doubles is greater than the 33-ft doubles, followed by the 48-ft doubles, due to the longer wheelbase providing additional lateral stability. However, as the speed continues to increase, the three curves of the A-doubles approach each other, and the opposite result appears. This is mainly because, at relatively high speeds, the trailer avoidance capacity (chance of the last trailer collision with the obstacle) that is discussed in Section 4.1 plays a more important role in affecting the LPTS than the roll and yaw motion limits.

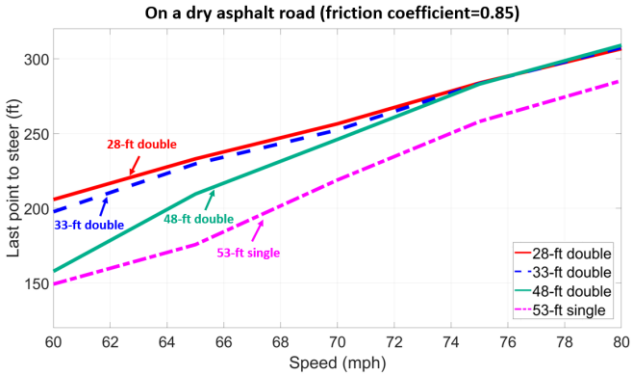

Figure 25. Comparison of the last point to steer among the combination vehicles at various speeds (on a dry asphalt road, friction coefficient = 0.85)

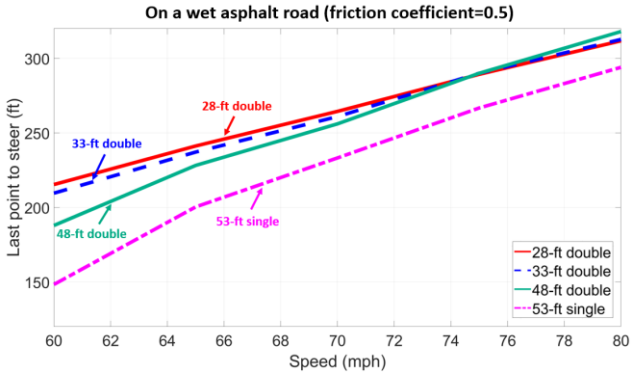

Figure 26. Comparison of the last point to steer among the combination vehicles at various speeds (on a wet asphalt road, friction coefficient = 0.5)

Figures 27 and 28 compare the evasive time among the selected combination vehicles for the dry and wet asphalt road conditions, respectively. The result trends are quite similar to those in Figures 25 and 26. As observed, the evasive time is dependent on speed, i.e. at higher speeds at which the vehicle travels, the more evasive time it needs in emergency evasive maneuvering. As compared to the dry road, the wet road results in a slight increase in the evasive time. In addition, the 28-ft doubles has the evasive time ranging from 2.3s to 2.6s for entire speed cases, which is 6%-31% larger than those of the 53-ft single. At speeds below 76 mph for the dry road and 75 mph for the wet road, the evasive time of the 28-ft doubles is larger than that of the 33-ft doubles, followed by the 48-ft doubles. In the same manner of evasive distance results, an opposite result is obtained for higher speeds, since the longer wheelbase causes more difficulty in avoiding the obstacle in the last trailer.

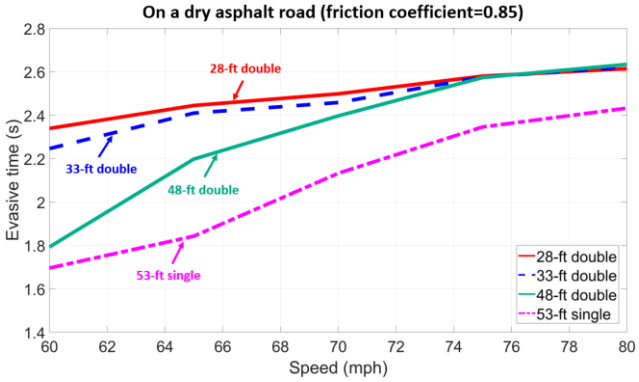

Figure 27. Comparison of the evasive time among the combination vehicles at various speeds (on a dry asphalt road, friction coefficient = 0.85)

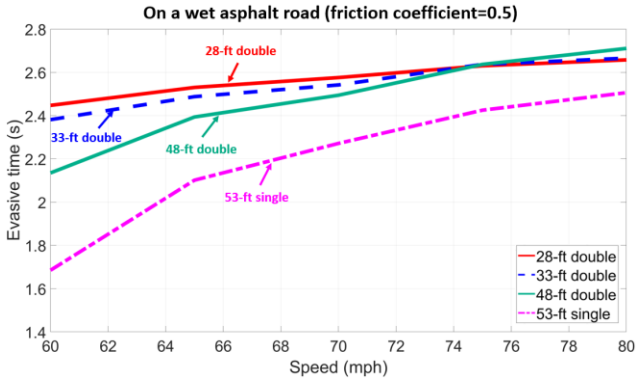

Figure 28. Comparison of the evasive time among the combination vehicles at various speeds (on a wet asphalt road, friction coefficient = 0.5)

5. Conclusions

A simulation-based analysis of the distance and time needed for long combination vehicles were provided for 28-, 33-, and 48-ft A-double trailers, using TruckSim®. The study mainly considered safely exercising an emergency, evasive steering maneuver, commonly required for obstacle avoidance at highway speeds. The last point to steer (LPTS) and evasive time (ET) at various highway speeds for A-double trailer results were compared with conventional tractor-semitrailers with a single 53-ft trailer for both dry and wet road conditions. It was determined that that the minimum distance and time required for obstacle avoidance of the 28-ft doubles various from 206 ft (60 mph) to 312 ft (80 mph) and 2.3s to 2.6s, respectively. In practice, as much as twice the theoretical times and distances that are presented in this study are needed to account for any vehicle (steering, etc.) and driver response delays. Such delays were not included here since different studies assume a range of delays for the driver response and steering response depending on a host of factors.

The results for LPTS represented a 6 to 31% increase for A-double trailers when compared with 53-ft semitrucks. At speeds below 76 mph on a dry road and below 75 mph on a wet road, the 28-ft doubles exhibited larger LPTS and ET than 33-ft doubles. In addition, the 33-ft doubles exhibited larger LPTS and ET than 48-ft doubles, due to the shorter trailers having a higher rear amplification. At higher speed (>75mph), however, this trend reverses. As the trailer length increases, the distance and time needed to safely avoid an obstacle also increase. The simulation results showed an increase in distance and time for obstacle avoidance on wet road conditions, as compared with dry roads.

References

[1] F. M. C. S. Administration, "Large Truck and Bus Crash Facts 2017," 2017. [Online]. Available: https://www.fmcsa.dot.gov/safety/data-and-statistics/large-truck-and-bus-crash-facts-2017.

[2] I. I. f. H. S. a. H. L. D. Institute. "Fatality Facts 2017-Large Trucks." https://www.iihs.org/topics/fatality-statistics/detail/large-trucks (accessed 10/03, 2019).

[3] Z. Shiller and S. Sundar, "Emergency lane-change maneuvers of autonomous vehicles," *ASME Journal of Dynamic Systems, Measurement and Control*, vol. 120, no. 1, pp. 37-44, 1998.

[4] T. Dang, J. Desens, U. Franke, D. Gavrila, L. Schäfers, and W. Ziegler, "Steering and evasion assist," *Handbook of intelligent vehicles*, pp. 759-782, 2012.

[5] A. Eckert, B. Hartmann, M. Sevenich, and P. Rieth, "Emergency steer & brake assist: a systematic approach for system integration of two complementary driver assistance systems," in *22nd International Technical Conference on the Enhanced Safety of Vehicles (ESV)*, 2011, pp. 13-16.

[6] A. Tamke, T. Dang, and G. Breuel, "A flexible method for criticality assessment in driver assistance systems," in *2011 IEEE Intelligent Vehicles Symposium (IV)*, 2011: IEEE, pp. 697-702.

[7] C. Ackermann, R. Isermann, S. Min, and C. Kim, "Collision avoidance with automatic braking and swerving," *IFAC proceedings volumes*, vol. 47, no. 3, pp. 10694-10699, 2014.

[8] R. Happee, C. Gold, J. Radlmayr, S. Hergeth, and K. Bengler, "Take-over performance in evasive manoeuvres," *Accident Analysis & Prevention*, vol. 106, pp. 211-222, 2017.

[9] R. Van Der Horst and J. Hogema, "Time-to-collision and collision avoidance systems," 1993.

[10] K. Vogel, "A comparison of headway and time to collision as safety indicators," *Accident analysis & prevention*, vol. 35, no. 3, pp. 427-433, 2003.

[11] A. Grislis, "Longer combination vehicles and road safety," *Transport*, vol. 25, no. 3, pp. 336-343, 2010.

[12] I. :, "Road vehicles–vehicle dynamics and road-holding ability–vocabulary," ed: International Organization for Standardization Geneva, 2011.

[13] Q. Wang and Y. He, "A study on single lane-change manoeuvres for determining rearward amplification of multi-trailer articulated heavy vehicles with active trailer steering systems," *Vehicle System Dynamics*, vol. 54, no. 1, pp. 102-123, 2016.

[14] Y. Chen, A. W. Peterson, C. Zhang, and M. Ahmadian, "A simulation-based comparative study on lateral characteristics of trucks with double and triple trailers," *International journal of vehicle safety*, vol. 11, no. 2, pp. 136-157, 2019.

[15] C. B. Winkler, "Rollover of heavy commercial vehicles," Society of Automotive Engineers, Warrendale, Pa., 1999.

[16] C. C. MacAdam, "Rearward amplification suppression (rams)," 2000.

[17] C. de Saxe and D. Cebon, "Estimation of trailer off-tracking using visual odometry," *Vehicle System Dynamics*, vol. 57, no. 5, pp. 752-776, 2019.

[18] S. Kharrazi, M. Lidberg, and J. Fredriksson, "Robustness analysis of a steering-based control strategy for improved lateral performance of a truck-dolly-semitrailer,"

International Journal of Heavy Vehicle Systems, vol. 22, no. 1, pp. 1-20, 2015.

[19] G. Morrison and D. Cebon, "Combined emergency braking and turning of articulated heavy vehicles," *Vehicle system dynamics*, vol. 55, no. 5, pp. 725-749, 2017.

[20] M. M. Islam, Y. He, S. Zhu, and Q. Wang, "A comparative study of multi-trailer articulated heavy-vehicle models," *Proceedings of the Institution of Mechanical Engineers, Part D: Journal of Automobile Engineering*, vol. 229, no. 9, pp. 1200-1228, 2015.

[21] M. M. Islam, N. Fröjd, S. Kharrazi, and B. Jacobson, "How well a single-track linear model captures the lateral dynamics of long combination vehicles," *Vehicle system dynamics*, vol. 57, no. 12, pp. 1874-1896, 2019.

[22] Y. Chen, A. W. Peterson, and M. Ahmadian, "Achieving anti-roll bar effect through air management in commercial vehicle pneumatic suspensions," *Vehicle System Dynamics*, vol. 57, no. 12, pp. 1775-1794, 2019.

[23] P. Nilsson and K. Tagesson, "Single-track models of an A-double heavy vehicle combination," Chalmers University of Technology, 2014.

[24] U. DoT, "Comprehensive truck size and weight study," *Federeal Highway Administration, Washington, DC*, 2000.

[25] Y. Chen, Y. Hou, A. Peterson, and M. Ahmadian, "Failure mode and effects analysis of dual levelling valve airspring suspensions on truck dynamics," *Vehicle system dynamics*, vol. 57, no. 4, pp. 617-635, 2019.

[26] Y. Chen, Zheng, X., Peterson, A., Ahmadian, M., , "Simulation Evaluation on the Rollover Propensity of Multi-trailer Trucks at Roundabouts," *SAE technical paper*, 2020, Art no. 2020-01-5005, doi: 10.4271/2020-01-5005.

[27] K. Nam, S. Oh, H. Fujimoto, and Y. Hori, "Estimation of sideslip and roll angles of electric vehicles using lateral tire force sensors through RLS and Kalman filter approaches," *IEEE Transactions on Industrial Electronics*, vol. 60, no. 3, pp. 988-1000, 2012.

[28] L. Balderas, "Representation of truck tire properties in braking and handling studies: the influence of vertical load on side force characteristics. Final report," 1988.

[29] H. B. Pacejka and R. S. Sharp, "Shear force development by pneumatic tyres in steady state conditions: a review of modelling aspects," *Vehicle system dynamics*, vol. 20, no. 3-4, pp. 121-175, 1991.

[30] F. H. Adnimistration. "Compilation of Existing State Truck Size and Weight Limit Laws." https://ops.fhwa.dot.gov/freight/policy/rpt_congress/truck_sw_laws/index.htm (accessed Dec, 2019).

[31] G. Markkula, O. Benderius, and M. Wahde, "Comparing and validating models of driver steering behaviour in collision avoidance and vehicle stabilisation," *Vehicle system dynamics*, vol. 52, no. 12, pp. 1658-1680, 2014.

[32] D. o. transportation, "Temporary Barrier Guidance Manual," 2018. Accessed: Jan/04/2020. [Online]. Available: http://www.dot.state.mn.us/trafficeng/workzone/doc/Temporary%20Barrier%20Guidance%20Manual%20181129.pdf

[33] P. Sweatman, A. Germanchev, and R. Di Cristoforo, "Stability and On-road Performance of Multi-combination Vehicles with Air Suspension Systems–Stage 2 Project–Final Report," *Roaduser Systems Pty Ltd*, 2005.

[34] R. D. Ervin, "The influence of size and weight variables on the roll stability of heavy duty trucks," *SAE Transactions*, pp. 629-654, 1983.

[35] H. Yu, L. Güvenc, and Ü. Özgüner, "Heavy duty vehicle rollover detection and active roll control," *Vehicle system dynamics*, vol. 46, no. 6, pp. 451-470, 2008.

[36] M. Acosta, S. Kanarachos, and M. Blundell, "Road friction virtual sensing: a review of estimation techniques with emphasis on low excitation approaches," *Applied Sciences*, vol. 7, no. 12, p. 1230, 2017.

Abbreviations

LCV	Long combination vehicle	**LPTS**	Last point to steer
ESA	Emergency steer assist	**LPTB**	Last point to brake
TTS	Time to steer	**ET**	Evasive time
TTC	Time to collision	**3-D**	Three dimensional
CG	Center of gravity	**CAD**	Computer aided design
DOT	Department of Transportation	**UMTRI**	University of Michigan Transportation Research Institute
MLPG	Michelin Laurens Proving Grounds	**RI**	Rollover Index

Definitions

t_l	Steering loss time	d_d	The distance to the obstacle
a_y	Vehicle lateral acceleration	s_y	Lateral offset
m_i	Vehicle mass	V_{xi}	Vehicle longitudinal velocity
V_{yi}	Vehicle lateral velocity	β_i	Vehicle yaw angle
δ	Wheel steering angle	F_{1s}	Tire cornering force at the steering axle
F_{1ft}	Tire cornering force at the front drive axle	F_{1rt}	Tire cornering force at the rear drive axle
α_{1s}	Tire slip angle at the steering axle	α_{1ft}	Tire slip angle at the front drive axle
α_{1rt}	Tire slip angle at the rear drive axle	α_2	Tire slip angle at the front trailer axle
α_3	Tire slip angle at the dolly axle	α_4	Tire slip angle at the rear trailer axle
I_i	Vehicle yaw moment of inertia	a_i	The distance from vehicle CG to the front articulation point
c_i	The distance from vehicle CG to the rear articulation point	b_{1f}	The distance from tractor CG to the front drive axle
b_{1r}	The distance from tractor CG to the rear drive axle	F_2	Tire cornering force at the front trailer axle
F_3	Tire cornering force at the dolly axle	F_4	Tire cornering force at the rear trailer axle
b_2	The distance from CG to the axle for the front trailer	b_3	The distance from CG to the axle for the dolly
b_4	The distance from CG to the axle for the rear trailer	d_c	The distance from the steering start point to point C

Note: the subscript letter *i=1,2,3,4* denotes the tractor, the front trailer, the dolly, and the rear trailer

Semitruck	Semi-tractor-trailer Truck	**A-double**	Truck with double trailers connected by an A-dolly
28-ft doubles	28-ft double-trailer Truck	**Single-trailer truck**	The combination of a tractor unit and a semitrailer
Combination vehicle	The combining of a tractor unit with one or more trailers		

Appendix A

Table A1. Parameters for the 28-ft doubles dynamic model in Simulink used to validate the TruckSim model

Tractor					
Variable	**Definition**	**Value**	**Variable**	**Definition**	**Value**
m_1	Vehicle mass	19300.0 lb	I_1	Yaw moment of inertia	488202.0 lb· ft^2
a_1	The distance from CG to the steering axle	129.6 in	b_{1f}	The distance from CG to the front drive axle	99.6 in
b_{1r}	The distance from CG to the rear drive axle	150.0 in	c_1	The distance from CG to the fifth-wheel	117.6 in
Front Trailer (same to rear trailer)					
Variable	**Definition**	**Value**	**Variable**	**Definition**	**Value**
m_2	Vehicle mass	16500.0 lb	I_2	Yaw moment of inertia	1437869.0 lb·ft^2
a_2	The distance from CG to the kingpin	157.2 in	b_2	The distance from CG to the axle	118.8 in
c_2	The distance from CG to the hitch	148.8 in		Trailer load	6000.0 lb
Dolly					
Variable	**Definition**	**Value**	**Variable**	**Definition**	**Value**
m_3	Vehicle mass	2600.0 lb	I_3	Yaw moment of inertia	41647.0 lb· ft^2
a_3	The distance from CG to the hitch	72.0 in	b_3	The distance from CG to the axle	1.0 in
c_3	The distance from CG to the fifth-wheel	2.0 in			

Table A2. Parameters for the tractor and dolly dynamics simulation in TruckSim

Vehicle unit	Parameter	Value
Tractor	Tractor sprung weight	14559.0 lb
	Roll moment of inertia	168436.0 lb·ft^2
	Pitch moment of inertia	539261.0 lb· ft^2
	Yaw moment of inertia	488202.0 lb· ft^2
	Wheelbase	253.0 in
	Steering axle track	80.0 in
	Drive axle track	73.5 in
	Longitudinal distance from CG to steer axle	128.6 in
	CG height to the ground	39.8 in
	Steering axle suspension stiffness	12197.0 lb/ft
	Steering axle suspension damping coefficient	1199.0 lb·s/ft
	Steering axle suspension lateral span (springs)	32.5 in
	Steering axle suspension lateral span (dampers)	43.3 in
	Drive axle suspension damping coefficient	1980.0 lb·s/ft
	Drive axle suspension lateral span (springs)	30.0 in
	Drive axle suspension lateral span (dampers)	42.0 in
	Steering ratio	22.0
	Fifth-wheel height to the ground	43.3 in
	Fifth-wheel roll freedom	±1 deg
	Fifth-wheel pitch freedom	-15 ~ 11 deg
	Fifth-wheel yaw freedom	±180 deg
	Steering axle unsprung weight	1256.6 lb
	Drive axle unsprung weight	1730.6 lb
A-dolly	Dolly sprung weight	1329.0 lb
	Roll moment of inertia	28476.0 lb· ft^2
	Pitch moment of inertia	35596.0 lb· ft^2
	Yaw moment of inertia	41647.0 lb· ft^2
	CG height to ground	35.4 in
	Longitudinal distance from CG to hitch	70.9 in
	Dolly unsprung weight (each axle)	1411.0 lb
	Suspension lateral spacing	34.0 in
	Damper lateral spacing	31.0 in
	Dolly fifth-wheel height to ground	43.3 in

Table A3. Parameters for the semi-trailer dynamics simulation in TruckSim

Trailer parameters	28-ft double	33-ft double	48-ft double	53-ft single
Truck gross weight (total)	80.0 kips	80.0 kips	80.0 kips	80.0 kips
Trailer tare weight	10.5 kips	11.5 kips	13.5 kips	17.0 kips
Empty trailer roll moment of inertia	138331 lb·ft^2	163424 lb·ft^2	190056 lb·ft^2	274660 lb·ft^2
Empty trailer pitch moment of inertia	1020147 lb·ft^2	1317863 lb·ft^2	4055518 lb·ft^2	4501663 lb·ft^2
Empty trailer yaw moment of inertia	978136 lb·ft^2	1292845 lb·ft^2	3978537 lb·ft^2	4388608 lb·ft^2
Load weight (each trailer)	18.5 kip	17.5 kip	14.0 kips	43.7 kips
Load volume/trailer capacity	80.0%	80.0%	80.0%	80.0%
Empty trailer CG height to the ground	67.0 in	67.0 in	67.0 in	67.0 in
Loaded trailer CG height to the ground	81.3 in	80.4 in	75.4 in	83.5 in
Longitudinal distance from loaded trailer CG to kingpin	137 in	167 in	256 in	285 in
Wheelbase	276 in	331 in	486 in	522 in